

Adversarial Transfer of Pose Estimation Regression

Boris Chidlovskii, Assem Sadek

Naver Labs Europe, chemin Maupertuis 6, Meylan-38240, France
firstname.lastname@naverlabs.com

Abstract. We address the problem of camera pose estimation in visual localization. Current regression-based methods for pose estimation are trained and evaluated scene-wise. They depend on the coordinate frame of the training dataset and show a low generalization across scenes and datasets. We identify the dataset shift an important barrier to generalization and consider transfer learning as an alternative way towards a better reuse of pose estimation models. We revise domain adaptation techniques for classification and extend them to camera pose estimation, which is a multi-regression task. We develop a deep adaptation network for learning scene-invariant image representations and use adversarial learning to generate such representations for model transfer. We enrich the network with self-supervised learning and use the adaptability theory to validate the existence of scene-invariant representation of images in two given scenes. We evaluate our network on two public datasets, Cambridge Landmarks and 7Scene, demonstrate its superiority over several baselines and compare to the state of the art methods.

1 Introduction

Visual localization is the task of accurate camera pose estimation in a known scene. It is a fundamental problem in robotics and computer vision, with multiple applications in autonomous vehicles, structure from motion (SfM), simultaneous localization and mapping (SLAM), Augmented Reality (AR) and Mixed Reality (MR) [29].

Traditional structure-based methods find correspondences between local features extracted from an image by applying image descriptors like SIFT, SURF or ORB [20,25] and 3D geometry of the scene obtained from SfM; obtained 2D-3D matches allow to recover the 6-DoF camera pose. The 3D-based methods are very accurate, their main drawback is that they are scene-specific, i.e., a 3D model needs to be build for each new scene and updated every time the scene changes.

Representing a scene as a simple set of 2D pose-annotated images is more flexible [28,38]. On one side, it represents all information needed to infer the 3D scene geometry; on the other side, it can be easy updated by adding more images. 2D scene representation can be easy adapted to new scenes, comparing to 3D-based methods, and allows to deploy machine learning techniques.

PoseNet [16] was first to cast camera localization as a regression problem. The trained model learns a mapping from image to absolute pose which is dependent on the coordinate frame of the train set. Models learned on one scene's train set work well on the same scene's test set but fail on other scenes. A typical example is shown in Figure 1.a) which plots poses of OldHospital and KingsCollege scenes from Cambridge

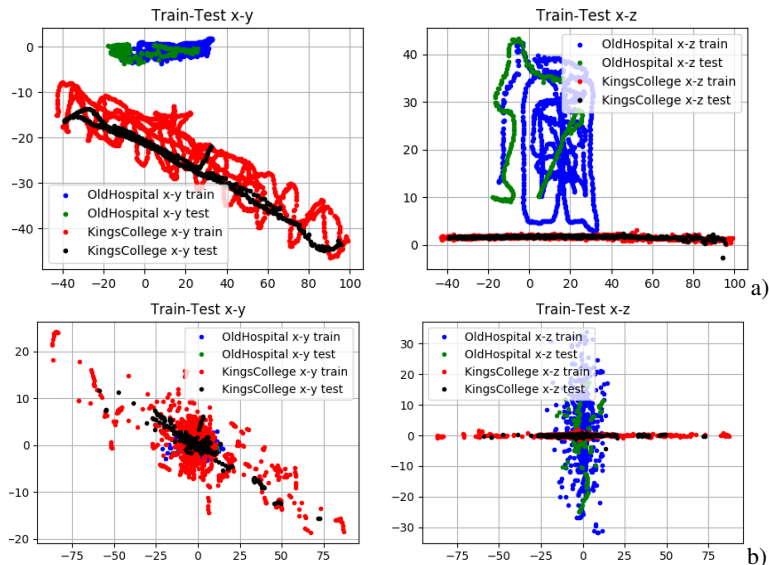


Fig. 1. Joint 2D projections of OldHospital and KingsCollege scenes, in position 3-DoF space. a) absolute poses; b) relative poses. Better seen in colors.

Landmarks dataset in the common coordinate frame. Absolute poses of the two scenes indeed differ in range and spread¹.

The problem of generalization is better addressed by relative pose regression [18]. Visual localization with relative poses commonly relies on image retrieval where a query image is compared against the database of images and its pose is inferred from poses of the retrieved images.

Multiple deep learning methods have been proposed to estimate the relative pose [1,18,23,24]. Relative poses indeed reduce the difference in range and spread but solve generalization to some extent only. Figure 1.b) demonstrates the phenomenon by plotting the two scenes' relative poses. 2D projections show that relative poses (blue and green vs red and black) are still sparse. Except the space origin, they still live in different segments of the 6D pose space. Being discriminative, the supervised regression model can not generalize to poses not seen in the train set [28].

State of the art methods, both 3D-based [35] and 2D-based [1,18,38] test with generalization by holding out one scene in Cambridge Landmarks and 7Scenes datasets for evaluation and training a relative pose model on the all remaining scenes. Concatenating multiple scenes allow to better populate the relative pose space and to reduce the dataset shift when testing the model on the evaluation scene.

However, this reduction is rather modest. Considering relative poses as 6D points, only 8.8% of relative poses in KingsCollege's test set (see Fig. 1.b) have a 1-top neighbour in OldHospital's train set. This fraction raises to merely 22.6% if the train set is a concatenation of OldHospital's, StMarysChurch's and ShopFacade's sets. Put all to-

¹ We show 3-DoF pose positions only; pose orientations show the same phenomenon.

gether, relative poses in Cambridge Landmark dataset occupy less than 7% of the 6D sphere with the radius equal to the average distance between two image poses. Taking the curse of dimensionality, many more annotated scenes are needed to densely populate the 6D relative pose space.

We argue that in order to progress in pose generalization one should take into account the *relative pose sparsity* and the *dataset shift* it provokes. One solution is to create a very large dataset (like ImageNet for image classification) by massively annotating scenes with poses. Such annotation is arduous and expensive, so the learner can deploy *multi-task learning* to optimize the performance across m tasks/scenes simultaneously, through some shared knowledge. However, this would not solve the output shift when testing the model on a new, unseen scene.

To cope with the dataset shift in pose estimation, we turn towards *transfer learning* and develop a method to transfer a pose model from one scene to another. Then we extend the method to process multiple scenes as input.

Domain adaptation. The lack of generalization is a fundamental problem in machine learning. Samples collected in different places and under different conditions results in the dataset bias when a learning method trained on one dataset generalizes poorly across other datasets [31].

Domain adaptation tries to produce good models on a target domain, by training on source labeled images and leveraging unlabeled target images as supplementary information during training. It has demonstrated a significant success in image classification [13], object recognition [22] and semantic segmentation [37]. These successes are due to a common semantic space shared by source and target domains. Common classes implicitly structure the output space [36], where separation between two classes in the source can be transferred to the target. Moreover this knowledge makes possible *unsupervised* domain adaptation [11,13,21].

Unlike classification, domain adaptation for multi-regression tasks is less studied [2,19]. Existing methods still assume the same output space and proceed by adjusting the loss function [10] or by reweighting source instances [8]. In camera pose estimation, one scene does correspond to one domain, but the difference in relative poses breaks the common space assumption. To extend domain adaptation to pose regression, we adopt the principle of domain-invariant representations [21] and use adversarial learning to generate such representations [6,7,11].

Due to the output shift, the source may have only some common poses with the target, so we need supplementary information about target pose space. In this paper we discuss *pose-driven* adaptation, where the transfer task is supported with a small number of target ground truth poses. With such a supplement, we learn scene-invariant representation of source and target images and pivot the source model towards the target.

As an additional contribution, we enrich pose regression with *self-supervised learning* which proved its efficiency in other vision tasks [12,17]. We apply random rotations [12] to an input image and train the network to predict these rotations. The method uses available training data to produce an additional self-supervision signal to the network and allows to learn a more accurate model.

2 Related work

Traditional structure-based methods rely on SfM to associate 3D points with 2D images represented with their local descriptors. Matches between 2D points in an image and 3D points in the scene are then found by searching through the shared descriptor space. The descriptors can either be hand crafted (e.g., SIFT, SURF or ORB) or learned (e.g., SuperPoint) [20,25]. Given a set of 2D-3D matches, a n-point-pose (PnP) solver estimates candidate poses, and the best pose hypothesis is chosen using RANSAC. The estimated best pose is typically a subject of a further refinement.

PoseNet [16] modified the GoogLeNet architecture, are replaced softmax layers with fully connected (FC) layers to regress the pose. Absolute pose estimation (APE) relies on deep network encodings that are more robust to challenging changes in the scene such as lighting conditions and viewpoint. Comparing to 3D-based methods, a trained model requires less memory and has a constant inference time.

Multiple improvements to the PoseNet include new loss functions [15], adding Long-Short-Term-Memory (LSTM) layers [33], the geometric re-projection error [14], and additional data sources and sensor measurements [5]. Other proposals extend the Posenet-like networks with auxiliary learning [24,32]. They learn additional auxiliary tasks which share representations with absolute pose estimation in order to improve its learning. VLocNet [32] implemented the auxiliary learning approach by jointly learning absolute and relative pose estimations. Its extended version, VLocNet++[24], added semantic segmentation as a second auxiliary task.

DSAC [3] and DSAC++[4], combine the pose estimation with structure-based methods and local learning. In such a hybrid paradigm, methods rely on geometrical constraints and utilize a structure-based pipeline where the learning is focused on local computer vision tasks, such as 2D-3D matches.

Instead of working with position and orientation losses separately, [38] learns the relative pose models directly from essential matrices and combines them with geometric models. It attributes the failure of pose regression in competition with geometric methods to the inaccurate feature representation in the last network layer. In this paper we identify the dataset shift as an additional reason of low generalization.

In 3D-based models, generalization efforts count on 3D point clouds and their associations with the scene images. SANet [35] is a scene agnostic neural architecture for camera localization, where model parameters and scenes are independent from each other. The method constructs scene and query feature pyramids, deploys the 3D point clouds at different scales and proceeds with query-scene registration (QSR). It first estimates a scene coordinate map and then computes the camera pose.

Domain Adaptation. Domain adaptation considers the discrepancy between training and testing domains as a fundamental obstacle to generalization [21,34]. The state of the art approaches address the problem by learning domain-invariant feature representations through adversarial deep learning [7,11,36]. These methods encourage samples from different domains to be non-discriminative with respect to domain labels. Ganin et al. [11] uses a domain classifier to regularize the extracted features to be indiscriminate with respect to the different domains. They assumed the existence of a shared

feature space between domains where the distribution divergence is small. The domain-adversarial neural network can be integrated into the standard deep architecture to ensure that the feature distributions over the two domains are made similar.

Initially studied under the assumption of same classes in source and target domains [11], domain adaptation research has recently turned towards more realistic settings. The new extensions address *partial* domain adaptation [6], when the target domain does not include all source classes, *open set* [27] when target include new classes, and *universal* domain adaptation [38] which treat both cases jointly.

3 Camera Pose Regression

Given an RGB image $\mathbf{x} \in \mathbb{R}^{h \times w \times 3}$, our task is to predict the (absolute or relative) camera pose $\mathbf{p} = [\mathbf{t}, \mathbf{q}]$ given by position vector $\mathbf{t} \in \mathbb{R}^3$ and orientation quaternion $\mathbf{q}, \mathbf{q} \in \mathbb{R}^4$. The following loss function is used to train a pose regression network [15]

$$L_p(\hat{\mathbf{p}}, \mathbf{p}) = \|\mathbf{t} - \hat{\mathbf{t}}\|e^{-s_t} + s_t + \|\mathbf{q} - \hat{\mathbf{q}}\|e^{-s_q} + s_q, \quad (1)$$

where $\hat{\mathbf{p}} = [\hat{\mathbf{t}}, \hat{\mathbf{q}}]$, and $\hat{\mathbf{t}}$ and $\hat{\mathbf{q}}$ represent the predicted position and orientation, respectively, s_t and s_q are trainable parameters to balance both distances, and $\|\cdot\|$ is the l_1 norm.

All pose regression networks share three main components, namely, encoder, localizer and regressor [28,29]. Given an image \mathbf{x} , encoder E is a deep network that extracts visual feature vectors from \mathbf{x} , $f = E(\mathbf{x})$. The localizer then uses FC layers to map a visual feature vector to a localization feature vector. Finally, two separate connected layers are used to regress $\hat{\mathbf{t}}$ and $\hat{\mathbf{q}}$, respectively, giving the estimated pose $\hat{\mathbf{p}} = [\hat{\mathbf{t}}, \hat{\mathbf{q}}]$.

Existing variations of this architecture concern the encoder network (GoogleNet [16] and ResNet34 with global average pooling [5]), and the localizer (1 to 3 FC layers, 1 FC layer extended with 4 LSTMs [33], etc.). We use a configuration that includes the ResNet34 encoder, 1 FC layer localizer and trained with the pose regression loss in Eq.1.

Absolute pose estimation methods [14,15,33] work with the absolute poses \mathbf{p} . To get relative poses, we follow AnchorNet [26] and explicitly define a set of anchor points, which correspond to a subset of all training images in the network, we then estimate the pose of a test image with respect to these anchors.

3.1 Self-supervision

We extend our pose estimation network with self-supervised learning [12,17]. This concept proposes to learn image representations by training the network to recognize the geometric transformation applied to an input image. It first defines a set of discrete geometric transformations, then those geometric transformations are applied to each input image. The produced transformed images are fed to the model that is trained to recognize the transformation.

We follow [12] in defining the geometric transformations as the image rotations by 0, 90, 180, and 270 degrees. Unlike [12] where the CNN model is trained on the

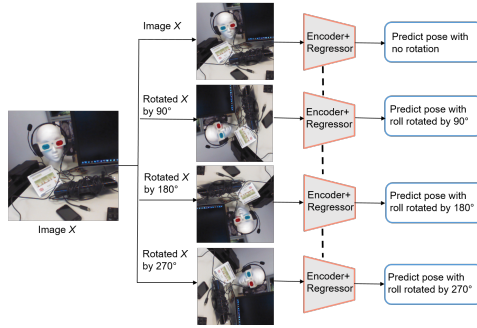


Fig. 2. Self-supervised learning by rotating the input images. The model learns to predict which rotation is applied.

4-way image classification task to recognize one of the four image rotations, we train the network to identify the rotation applied to the input image (see Figure 2). The main argument is that in order a CNN model to be able recognize the rotation transformation that was applied to an image it will require to understand the concept of the objects present in the image, such as their location and their pose [17].

We crop the input image and rotate it randomly 0, 90, 180 or 270 degrees and expect that the network is able to predict the rotation applied to the image.

Image rotation changes its orientation \mathbf{q} but not position \mathbf{t} . We calculate the orientation of the rotated image by first transforming the quaternion \mathbf{q} of the input image in Euler angles $yaw, pitch, roll$. Then, we change $roll$ accordingly to the applied rotation, and transform the new angles back in quaternion \mathbf{q}' . Fed with the rotated image, we train the network to predict pose of the rotated image to be $[\mathbf{t}, \mathbf{q}']$.

3.2 Adversarial Pose Adaptation Network

We now consider the task of adapting a pose regression model from one (source) scene to another (target) scene. The task constitutes a source set $D_s = \{(\mathbf{x}_s^i, \mathbf{p}_s^i)\}_{i=1}^{n_s}$ of n_s images with ground truth poses and a target set $D_t = \{\mathbf{x}_t^j\}_{j=1}^{n_t}$ of n_t images. A small number of target images might be labeled with poses, $D_t^a = \{(\mathbf{x}_t^j, \mathbf{p}_t^j)\}_{j=1}^{n_t^a}$, $n_t^a \ll n_t$. Unlike the classification and semantic segmentation, where source and target domains share the same classes, we additionally face the output shift, where source and target poses lie in different segments of the coordinate system, i.e. $\{\mathbf{p}_s\} \neq \{\mathbf{p}_t\}$.

Our pose adaptation network enables an end-to-end training of a transferable encoder E and an adaptive pose regressor G_p . Trained on labeled source images and (mostly) unlabeled target images, the network enables an accurate adaptation of the source pose model to the target scene.

The main problem of domain adaptation is to reduce the discrepancy between the source and target images [21]. Domain adversarial networks [7, 11, 36] tackle this problem by learning *scene-invariant* image representations in a two-player minimax game.

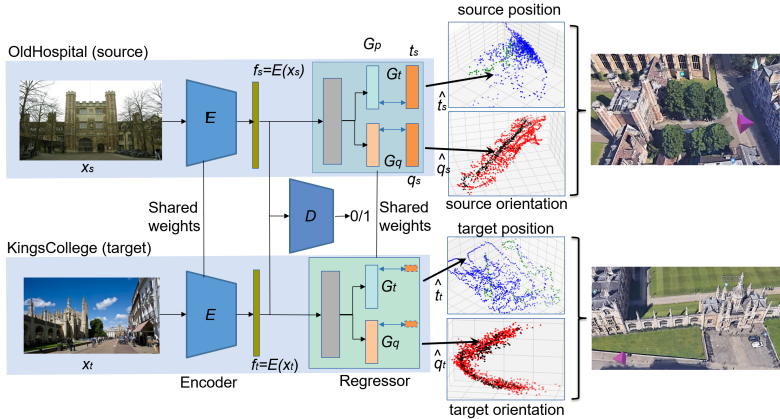


Fig. 3. Adversarial Pose Adaptation Network for the camera pose adaptation, where E is the transferable encoder, G_p is the adaptive pose regressor (including the localizer), D is scene discriminator.

The first player is a scene discriminator G_d trained to distinguish feature representations of source images from target images, and the second player is the encoder E trained simultaneously to deceive the domain discriminator G_d .

Specifically, the scene-invariant image representations $f = E(x)$ are learned in a minimax optimization procedure, where encoder E is trained by maximizing the loss of scene discriminator G_d , while G_d is trained by minimizing its own scene discrimination loss. As the ultimate goal is to learn a source pose regression model and transfer it to target scene, the loss of the source pose regressor G_p should be also minimized.

This leads to the optimization problem over the following terms.

Source pose regression. The source regression loss is defined on labeled source images,

$$\mathcal{L}_{pose}^s(E, G_p) = \sum_{\mathbf{x}_i \in D_s} L_p(G_p(E(\mathbf{x}_i)), \mathbf{p}_i), \quad (2)$$

where L_p is the regression loss function defined in Eq. 1.

Scene discrimination network. Scene discriminator G_d is trained to distinguish between feature representations of the source and target images, with the adversarial loss

$$\mathcal{L}_{adv}(G_d) = - \sum_{\mathbf{x}_i \in D_s \cup D_t} L_d(G_d(E(\mathbf{x}_i)), \mathbf{d}_i), \quad (3)$$

where L_d is the cross-entropy loss function and \mathbf{d}_i is the scene label (0 for source images and 1 for target images).

Semi-supervised adaptation. In classification, domain adaptation can be achieved with the two above terms in an unsupervised way [11,36]. In pose regression, we are supplied

with a small number of labeled target images, D_t^a . Then we define a regression term on D_t^a ,

$$\mathcal{L}_{pose}^t(E, G_p) = \sum_{\mathbf{x}_j \in D_t^a} L_p(G_p(E(\mathbf{x}_t^j)), \mathbf{p}_t^j), \quad (4)$$

where L_p is the regression loss function defined in Eq. 1. The pose regression loss then includes the source and target terms, $\mathcal{L}_{pose}(E, G_p) = \mathcal{L}_{pose}^s(E, G_p) + \mathcal{L}_{pose}^t(E, G_p)$.

The total loss for training our *adversarial pose adaptation network* (APANet) can be represented as

$$\mathcal{L}_{APANet}(E, G_p, G_d) = \mathcal{L}_{pose}(E, G_p) + \alpha \mathcal{L}_{adv}(E, G_d), \quad (5)$$

where α is a hyper-parameter controlling the importance of the adversarial loss.

The training objective of the minimax game is the following

$$E^*, G_p^* = \arg \min_{E, G_p} \max_{G_d} \mathcal{L}_{APANet}(E, G_d, G_p). \quad (6)$$

Eq. 6 is solved by alternating between optimizing E, G_p and G_d until the total loss (5) converges.

The APANet architecture is presented in Figure 3. The network inputs a batch of source images and a batch of target images. Encoder E generates image representations $f = E(\mathbf{x})$ for both batches. Scene discriminator G_d is trained on image representations f and scene labels \mathbf{d} to distinguish source images from target images. Pose regressor G_p is trained on a full set of source image poses and, when available, a small number of target scene poses. Position regressor G_t and orientation regressor G_q are trained separately. The position and orientation predictions are concatenated to produce the 6-DoF pose estimation, $\hat{\mathbf{p}} = [\hat{\mathbf{t}}, \hat{\mathbf{q}}]$, where $\hat{\mathbf{t}} = G_t(E(\mathbf{x}))$ and $\hat{\mathbf{q}} = G_q(E(\mathbf{x}))$.

3.3 Scene adaptability

We complete this section by the notion of adaptability which has been introduced [9] to measure the transferability of feature representations from one domain to another. Adaptability is quantified by the error of a joint hypothesis h^* in both domains. The ideal joint hypothesis h^* is found by training on both source and target labeled images. Note that the target labels are only used to reason about the adaptability.

If the joint model shows a low error on source and target test sets, it suggests that an efficient transfer is possible across domains. In the evaluation section, we apply this idea to pose adaptation tasks. We will learn a joint model in order to reason about adaptability of source absolute and relative models to the target scene.

4 Evaluation

Datasets. We test our pose adaptation network on two public datasets, Cambridge Landmarks [16] and 7Scene [30]. *Cambridge Landmarks* [16] is an outdoor dataset collected in four sites around Cambridge University. It is collected using a Google mobile phone while pedestrians walk. The images are captured at the resolution of 1920x1080,

the ground truth pose is obtained through VisualSFM software. Each site corresponds to one scene: Old Hospital, King’s College, StMary’s Church and Shop Facade. We first consider 1-to-1 scenario to test the model transfer from one scene to another. We form twelve pose adaptation tasks, by enumerating all possible *source* \rightarrow *target* pairs. Then, we consider n -to-1 scenario and form four adaptation tasks, where one scene is retained as target and three remaining scenes is used as source.

7Scene [30] is an indoor dataset collected with a handheld RGB-D camera. The ground truth pose is generated using the Kinect Fusion approach [30]. The dataset is captured in 7 indoor scenes. In 1-to-1, we form twelve adaptation tasks, with Chess selected as a pivot scene. It constitutes six Chess $\rightarrow X$ tasks and six $X \rightarrow$ Chess tasks, where X is one of the six remaining scenes: Fire, Heads, Office, Pumpkin, Red Kitchen or Stairs. In n -to-1 scenario, seven adaptation tasks are formed, one scene is retained as target and six other scenes is used as source.

Source	Case	Method	OldHospital	StMarysChurch	ShopFacade
Kings	3D	DSAC++ [4]	0.20/0.30	0.13/0.40	0.06/0.30
College	APE	No adaptation	38.63/83.04	28.53/110.39	31.21/45.19
		Joint	1.55/5.05	2.19/6.65	1.32/4.58
		SS, $\nu=0.05$	6.74/14.92	6.76/15.84	6.52/13.10
		APANet, $\nu=0.05$	3.74/8.27	3.63/10.18	2.61/8.63
		APANetS, $\nu=0.05$	3.56/6.71	3.58/8.23	2.58/7.41
	RPE	No adaptation	3.63/7.22	3.53/10.39	2.91/8.16
		Joint	0.53/1.59	0.45/1.21	0.42/1.29
		SS, $\nu=0.05$	1.54/1.82	1.36/3.04	1.18/3.81
		APANet, $\nu=0.05$	1.03/2.17	0.80/2.18	0.61/2.62
		APANetS, $\nu=0.05$	0.98/1.94	0.77/2.25	0.62/2.49
		NC-Essnet* [38]	0.95/2.65	1.12/3.64	0.70/3.41

Table 1. KingsCollege $\rightarrow X$ adaptation tasks in Cambridge Landmarks dataset. The median position (in meters) / orientation (in degrees) errors are reported.

Implementation and Setup. The APANet is implemented in PyTorch. Encoder E is fine-tuned on ResNet-34 network. Pose regressor G_p and scene discriminator G_d are trained from scratch. G_p includes a FC localizer with 1024 nodes and two separate layers G_t and G_q , to regress position and orientation vectors, with 256 nodes each. Scene discriminator G_d is similar to one used in the universal domain adaptation (UDA) network [36]; it includes three FC layers with 1024, 256 and 64 nodes, interleaved with ReLU layers, the drop-out is 0.5.

In the train phase, the network inputs a batch of source images and a batch of target images to fine-tune the encoder E and to train scene discriminator G_d and pose regressor G_p . In the test phase, only encoder E and pose regressor G_p are necessary. A target image \mathbf{x}_t is fed to the network and its pose is estimated as $G_p(E(\mathbf{x}_t))$.

We use the Adam optimizer; we train the network with a learning rate of 10^{-5} and the batch size of 16 images. We initialize parameters s_t and s_q in the pose loss (Eq. 1) with 0 and -1.0 respectively. Hyper-parameter α is set to 1.0. We use the same image pre-processing steps as the state of the art methods [15,28]. For training, we randomly

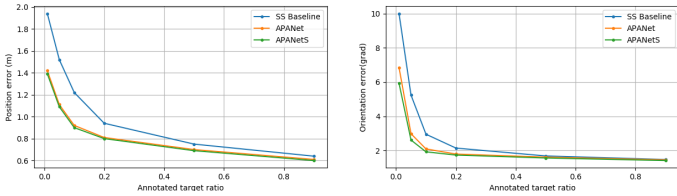


Fig. 4. Position (top) and orientation (bottom) RPE errors of SS, APANet and APANetS for different ν values.

crop the image to 224×224 pixels. For testing, images are cropped to 224×224 pixels at the center of the image. Training images are shuffled before they are fed to the network. In the self-supervised extension (APANetS), the input image is randomly rotated 0, 90, 180, 270 degrees and the network is trained to correctly predict the applied rotation.

Evaluation options. For all adaptation tasks, we compare five models, including two baselines and two APANet versions. First, we train the *joint model* (see Section 3.3) on source and target train sets. This model is an indicator of adaptability of the source model to target scene. The low error on source and target test sets suggests a good generalization and there exists a joint model performing well on both scenes. Second, as the true baseline, we consider a *semi-supervised (SS) relaxation* of the joint model, where a fraction of target train set is used for training. Denoted ν , where $\nu = \frac{n_t^a}{n_t}$, this fraction varies between 0 (source scene only) and 1 (the joint model).

The third model is the APANet (Section 3.2) trained with ν target poses. This model can be considered as the SS baseline extended with adversarial learning of scene-invariant image representations. Finally, we include results of APANet extended with *self-supervision* (Section 3.1) and denoted APANetS.

The joint model gives an estimate of the smallest error the optimal joint model could achieve on the target scene. It serves as an indicator for the SS baseline and APANets. All three methods are exposed to the trade-off between ratio ν and accuracy drop with respect to the joint model. In the following, we compare the SS baseline and APANets for the same values of ν , in order to measure the size of target supplement sufficient to ensure an efficient pose mode transfer.

4.1 Evaluation Results

Cambridge Landmarks. Table 1 reports APE and RPE evaluation results for three adaptation tasks KingsCollege $\rightarrow X$. For each task, the table reports the error without adaptation, the joint model error, SS and APANets errors for the selected value $\nu = 0.05$, which corresponds to 5% of target ground truth poses available for training. In all tasks, the joint model error is small and suggests a good adaptability across scenes.

For the ratio $\nu = 0.05$, APANets perform much better than the SS baseline. Averaged over 12 adaptation tasks, the APANet position error is 46.8% (APE) and 52.2% (RPE) lower than the SS position error. Similarly, the APANet orientation error is on

average 37.9% and 42.1% lower than the SS orientation error. Self-supervised image rotation in APANetS further reduces the orientation error but has a negligible impact on the position error.

Source	Case	Method	Fire	Heads	Office	Pumpkin	Kitchen	Stairs
Chess	3D	DSAC++ [4]	0.02/0.90	0.01/0.80	0.03/0.70	0.04/1.10	0.04/1.10	0.09/2.60
		APE	2.25/28.32	1.91/31.76	0.30/23.75	1.08/20.82	1.59/23.14	1.83/28.45
	APE	Joint	0.40/9.45	0.28/14.41	0.31/7.20	0.27/4.91	0.34/7.26	0.34/9.52
		SS, $\nu=0.05$	1.31/19.08	1.04/24.62	0.89/18.36	0.82/11.15	1.01/17.59	1.03/20.12
		APANet, $\nu=0.05$	0.63/14.67	0.44/17.03	0.42/10.62	0.39/6.87	0.43/10.35	0.47/12.28
		APANetS, $\nu=0.05$	0.59/12.06	0.41/14.29	0.41/8.45	0.37/5.71	0.41/8.66	0.48/9.87
		No Adaptation	2.25/28.32	1.91/31.76	1.63/23.75	2.78/20.82	1.89/23.14	1.83/28.45
		Joint	0.11/7.14	0.08/7.14	0.09/4.02	0.09/4.68	0.07/3.86	0.09/8.52
	RPE	SS, $\nu=0.05$	0.41/17.08	0.34/14.62	0.29/14.36	0.42/11.15	0.31/7.75	0.29/19.12
		APANet, $\nu=0.05$	0.22/10.15	0.17/10.26	0.14/7.36	0.19/6.46	0.19/5.65	0.17/12.28
		APANetS, $\nu=0.05$	0.21/9.72	0.15/9.35	0.15/6.69	0.19/5.87	0.16/5.13	0.16/11.77
		NC-EssNet* [38]	0.26/9.64	0.14/10.66	0.20/6.68	0.22/5.72	0.22/6.31	0.31/17.88

Table 2. 1-to-1 transfer in 7Scenes dataset. The median position (in meters) / orientation (in degrees) errors are reported.

Impact of ratio ν . Figure 4.1 gives an aggregated view by averaging results over twelve adaptation tasks. It compares the SS, APANet and APANetS errors for ν varying between 0.01 and 0.90.

The figure shows little or no difference when target poses are abundantly available in training. Having 20% or more target poses is sufficient to train a joint model working well on both scenes. Instead, when the ratio ν is reduced to 1%-5%, the advantage of APANet over the SS baseline becomes multi-fold. We conclude that learning scene-invariant image representations accelerates the adaptation across scenes. Moreover it enables an accurate adaptation with a smaller target supplement.

Note no existing RPE method can perform 1-to-1 scenario without performance drop. Results for 3D-based DSAC++ [4] and 2D-based NC-EssNet [38] are included in Table 1 (and Table 2) for the comparison only. The state of the art NC-EssNet is a supervised learning method trained and tested on the target scene, while APANet(S) are transfer models trained on the source train set and a fraction of the target train set. Still, all 2D-based methods are less accurate than the best 3D-based models, such as DSAC++ and Active Search.

7Scenes. Table 2 reports evaluation results for 1-to-1 adaptation tasks Chess $\rightarrow X$ in the 7Scene dataset. In all tasks, we again observe a small error of the joint models. For the ratio $\nu = 0.05$, the APANet performs better than the SS baseline and APANetS improves over APANet in the orientation error.

Cross dataset transfer. Table 3 reports evaluation results for 1-to-1 and n -to-1 scenarios, on the same or across the Cambridge and 7Scenes datasets. When we test the APANets in n -to-1 scenario on the same dataset, a model is trained with all but one scenes, such a setup is used in the previous methods [18,38]. In evaluations across

Source	Target	Case	Joint	SS, $\nu=0.05$	Apanet, $\nu=0.05$	APANetS, $\nu=0.05$	NC-EssNet*
Cambridge	Cambridge	1-to-1	0.67/1.45	1.90/4.08	0.88/3.07	0.87/2.86	0.85/2.82
		n-to-1	0.63/1.38	1.51/3.82	0.81/2.96	0.82/2.56	
Cambridge	7Scenes	1-to-1	0.36/6.37	1.13/20.10	0.62/13.16	0.61/12.43	0.48/32.97
		n-to-1	0.31/6.49	1.19/19.01	0.50/13.47	0.47/12.96	
7Scenes	7Scenes	1-to-1	0.13/3.84	0.38/10.22	0.25/7.63	0.24/7.16	0.21/7.50
		n-to-1	0.13/3.45	0.34/9.30	0.22/7.76	0.22/7.31	
7Scenes	Cambridge	1-to-1	1.78/7.42	5.86/27.17	3.95/16.67	3.91/16.15	7.98/24.35
		n-to-1	1.61/7.55	5.81/26.08	3.86/15.86	3.87/15.56	

Table 3. RPE transfer in 1-to-1 and n-to-1 scenarios. The median position (in meters) / orientation (in degrees) errors are reported.

the two datasets, all scenes from the source dataset are used for training. All the joint models behave well and indicate a good generalization. The self-supervised learning in APANetS reduces the orientation error. Instead, adding more scenes does really help APANet and APANetS.

Again, results of NC-EssNet [38] are included for the comparison only. Being totally supervised, NC-EssNet shows good performance on the same dataset (Cambridge to Cambridge and 7Scenes to 7Scenes) but suffers from the dataset shift in the cross-dataset evaluations, if compared with APANets.

4.2 Discussion

We identify the dataset shift an important barrier to the generalization of pose estimation models. Analysis of the evaluation results in the previous section raises two critical issues. One concerns the target supplement to accompany the adaptation process and to preserve the pose estimation accuracy. We have promoted the pose-driven adaptation, where a small number of target poses guide adaptation with a modest performance drop. This method showed promising results. However, acquiring target ground truth poses is not always possible. We therefore need alternatives to parametrize the model transfer across scenes, where a model-driven regression can alleviate the absence of target poses.

Another issue concerns scene adaptability. Low joint model errors in both datasets have been a strong indicator that the pose regression adaptation is possible and the scene-invariant representations can accelerate the adaptation process. If, instead, the joint model error is higher, it can seriously compromise any chances of an efficient adaptation. In the Cambridge Landmarks dataset, the joint models for the lately added Street scene indeed show a high error. This suggests a low adaptability from and to Street scene. The adaptability theory developed an instance adaptation technique for low adaptability in classification tasks [9]. Therefore it looks important to extend this theory to multi-regression tasks as well.

5 Conclusion

We address the problem of low generalization of the relative pose estimation models. We attribute it to the dataset shift and propose adaptation across scenes as an alternative

way towards a better generalization. We extend domain adaptation techniques invented for classification to the multi-regression task and developed a deep network to adapt a pose regression model from one scene to another. The Adversarial Pose Adaptation Network learns scene-invariant image representations and use target scene supplements to guide the transfer of source models to the target scene. We also use the adaptability theory to measure the transferability of feature representations from one scene to another. We validate the superiority of the APANet on Cambridge Landmarks and 7Scene datasets over the baselines and compare them to the state of the art supervised methods.

References

1. Balntas, V., Li, S., Prisacariu, V.: Relocnet: Continuous metric learning relocalisation using neural nets. In: European Conference Computer Vision (ECCV). pp. 782–799 (2018)
2. Borchani, H., Varando, G., Bielza, C., Larrañaga, P.: A survey on multi-output regression. *Wiley Int. Rev. Data Min. and Knowl. Disc.* **5**(5), 216–233 (2015)
3. Brachmann, E., Krull, A., Nowozin, S., Shotton, J., Michel, F., Gumhold, S., Rother, C.: DSAC - differentiable RANSAC for camera localization. In: Computer Vision Pattern Recognition (CVPR). pp. 2492–2500 (2017)
4. Brachmann, E., Rother, C.: Learning less is more - 6d camera localization via 3d surface regression. In: Computer Vision Pattern Recognition (CVPR). pp. 4654–4662 (2018)
5. Brahmabhatt, S., Gu, J., Kim, K., Hays, J., Kautz, J.: Geometry-aware learning of maps for camera localization. In: Computer Vision Pattern Recognition (CVPR). pp. 2616–2625 (2018)
6. Cao, Z., Ma, L., Long, M., Wang, J.: Partial adversarial domain adaptation. In: European Conference Computer Vision (ECCV). pp. 139–155 (2018)
7. Cao, Z., You, K., Long, M., Wang, J., Yang, Q.: Learning to transfer examples for partial domain adaptation. In: Computer Vision Pattern Recognition (CVPR). pp. 2985–2994 (2019)
8. Chen, X., Monfort, M., Liu, A., Ziebart, B.D.: Robust covariate shift regression. In: Proc. AISTATS. vol. 51, pp. 1270–1279 (2016)
9. Chen, X., Wang, S., Long, M., Wang, J.: Transferability vs. discriminability: Batch spectral penalization for adversarial domain adaptation. In: Intern. Conference Machine Learning (ICML). vol. 97, pp. 1081–1090 (2019)
10. Cortes, C., Mohri, M.: Domain adaptation in regression. In: Proc. 22nd Intern. Conf. on Algorithmic Learning Theory (2011)
11. Ganin, Y., Ustinova, E., Ajakan, H., Germain, P., Larochelle, H., Laviolette, F., Marchand, M., Lempitsky, V.S.: Domain-adversarial training of neural networks. *J. Mach. Learn. Res.* **17**, 59:1–59:35 (2016)
12. Gidaris, S., Singh, P., Komodakis, N.: Unsupervised representation learning by predicting image rotations. In: iclr (2018)
13. Hoffman, J., Rodner, E., Donahue, J., Darrell, T., Saenko, K.: Efficient learning of domain-invariant image representations. *CoRR arXiv:1301.3224* (2013)
14. Kendall, A., Cipolla, R.: Modelling uncertainty in deep learning for camera relocalization. In: IEEE International Conference on Robotics and Automation, ICRA. pp. 4762–4769 (2016)
15. Kendall, A., Cipolla, R.: Geometric Loss Functions for Camera Pose Regression with Deep Learning. In: Computer Vision Pattern Recognition (CVPR). pp. 6555–6564 (2017)
16. Kendall, A., Grimes, M., Cipolla, R.: PoseNet: A Convolutional Network for Real-Time 6-DOF Camera Relocalization. In: Intern. Conference Computer Vision (ICCV). pp. 2938–2946 (2015)

17. Kolesnikov, A., Zhai, X., Beyer, L.: Revisiting self-supervised visual representation learning. In: *cvpr*. pp. 1920–1929 (2019)
18. Laskar, Z., Melekhov, I., Kalia, S., Kannala, J.: Camera Relocalization by Computing Pairwise Relative Poses Using Convolutional Neural Network. In: *IEEE International Conference on Computer Vision Workshops*. pp. 929–938 (2017)
19. Lathuilière, S., Mesejo, P., Alameda-Pineda, X., Horaud, R.: A comprehensive analysis of deep regression. *CoRR* **1803.08450** (2018)
20. Leng, C., Zhang, H., Li, B., Cai, G., Pei, Z., He, L.: Local feature descriptor for image matching: A survey. *IEEE Access* **7**, 6424–6434 (2019)
21. Long, M., Cao, Y., Wang, J., Jordan, M.I.: Learning transferable features with deep adaptation networks. In: *Intern. Conference Machine Learning (ICML)*. pp. 97–105 (2015)
22. Long, M., Wang, J., Ding, G., Sun, J., Yu, P.S.: Transfer joint matching for unsupervised domain adaptation. In: *Computer Vision Pattern Recognition (CVPR)*. pp. 1410–1417 (2014)
23. Melekhov, I., Ylioinas, J., Kannala, J., Rahtu, E.: Relative Camera Pose Estimation Using Convolutional Neural Networks. *CoRR* **1702.01381** (2017)
24. Radwan, N., Valada, A., Burgard, W.: Vlocnet++: Deep multitask learning for semantic visual localization and odometry. *IEEE Robotics and Automation Letters* **3**(4), 4407–4414 (2018)
25. Rublee, E., Rabaud, V., Konolige, K., Bradski, G.R.: ORB: an efficient alternative to SIFT or SURF. In: *Intern. Conference Computer Vision (ICCV)*. pp. 2564–2571 (2011)
26. Saha, S., Varma, G., Jawahar, C.V.: Improved visual relocalization by discovering anchor points. In: *British Machine Computer Vision (BMVC)*. p. 164 (2018)
27. Saito, K., Yamamoto, S., Ushiku, Y., Harada, T.: Open set domain adaptation by backpropagation. In: *European Conference Computer Vision (ECCV)*. pp. 153–168 (2018)
28. Sattler, T., Zhou, Q., Pollefeys, M., Leal-Taixe, L.: Understanding the Limitations of CNN-based Absolute Camera Pose Regression. In: *Computer Vision Pattern Recognition (CVPR)*. pp. 3302–3312 (2019)
29. Shavit, Y., Ferens, R.: Introduction to Camera Pose Estimation with Deep Learning. *CoRR* **1907.05272** (2019)
30. Shotton, J., Glocker, B., Zach, C., Izadi, S., Criminisi, A., Fitzgibbon, A.W.: Scene coordinate regression forests for camera relocalization in RGB-D images. In: *Computer Vision Pattern Recognition (CVPR)*. pp. 2930–2937 (2013)
31. Torralba, A., Efros, A.A.: Unbiased look at dataset bias. In: *Computer Vision Pattern Recognition (CVPR)*. pp. 1521–1528 (2011)
32. Valada, A., Radwan, N., Burgard, W.: Deep auxiliary learning for visual localization and odometry. In: *IEEE International Conference on Robotics and Automation, ICRA*. pp. 6939–6946 (2018)
33. Walch, F., Hazirbas, C., Leal-Taixé, L., Sattler, T., Hilsenbeck, S., Cremers, D.: Image-based localization using lstms for structured feature correlation. In: *Intern. Conference Computer Vision (ICCV)*. pp. 627–637 (2017)
34. Wang, M., Deng, W.: Deep visual domain adaptation: A survey. *Neurocomputing* **312**, 135–153 (2018)
35. Yang, L., Bai, Z., Tang, C., Li, H., Furukawa, Y., Tan, P.: Sanet: Scene agnostic network for camera localization. In: *European Conference Computer Vision (ECCV)*. pp. 42–51 (2019)
36. You, K., Long, M., Cao, Z., Wang, J., Jordan, M.I.: Universal Domain Adaptation. In: *Computer Vision Pattern Recognition (CVPR)*. pp. 2720–2729 (2019)
37. Zhang, Y., David, P., Gong, B.: Curriculum domain adaptation for semantic segmentation of urban scenes. In: *Intern. Conference Computer Vision (ICCV)*. pp. 2039–2049 (2017)
38. Zhou, Q., Sattler, T., Pollefeys, M., Leal-Taixe, L.: To learn or not to learn: Visual localization from essential matrices. *CoRR* **abs/1908.01293** (2019)